Finite-temperature coherence and entanglement in asymmetric bosonic Josephson junctions

Luca Salasnich*

in collaboration with

M. Ferraretto and C. Vianello

*Dipartimento di Fisica e Astronomia "Galileo Galilei", Università di Padova,
INFN, Sezione di Padova,
INO-CNR, Unita di Sesto Fiorentino (Firenze)

Classical and Quantum Complexity in Statistical Mechanics,
Molveno (Trento), July 21, 2025

Summary

- Two-site Bose-Hubbard model
- Semiclassical approximation
- Semiclassical approximation at finite temperature
- Exact diagonalization: Thermal equilibrium
- Coherence visibility: Exact vs semiclassical
- Population imbalance: Exact vs semiclassical
- Entanglement entropy: Exact without semiclassical
- Conclusions

Two-site Bose-Hubbard model

A system of N interacting bosons confined by an asymmetric double-well potential can be described by the two-site Bose-Hubbard model

$$\hat{H} = -J(\hat{a}_L^\dagger \hat{a}_R + \hat{a}_R^\dagger \hat{a}_L) + \frac{U}{2}[\hat{N}_L(\hat{N}_L - 1) + \hat{N}_R(\hat{N}_R - 1)] + \frac{\varepsilon}{2}(\hat{N}_L - \hat{N}_R) \quad (1)$$

with $J > 0$ the tunneling (hopping) energy, U the boson-boson interaction, and ε the on-site energy asymmetry.

The mean-field approximation is obtained by using **Glauber coherent states**

$$|\psi(t)\rangle = |\alpha_L(t)\rangle_L |\alpha_R(t)\rangle_R \quad (2)$$

where $|\alpha_j\rangle$ is the eigenstate of the annihilation operator $\hat{a}_j$, with complex eigenvalue

$$\alpha_j(t) = \sqrt{N_j(t)}\, e^{i\theta_j(t)} \quad (3)$$

where $N_j(t) = \langle \hat{N}_j \rangle$ is the average number of bosons in the site $j = L, R$ and $\theta_j(t)$ is the corresponding phase.

Two site Bose-Hubbard model

One can also introduce[1] the **relative phase**

$$\theta(t) = \theta_R(t) - \theta_L(t) \tag{4}$$

and the normalized **population imbalance**

$$z(t) = \frac{N_L(t) - N_R(t)}{N} \qquad \in [-1, 1] \, . \tag{5}$$

Here $N = N_L(t) + N_R(t)$ is a constant of motion.
Quite remarkably, $z(t)$ is canonically conjugate to $\theta(t)$. In particular, defining the canonical momentum

$$p_\theta(t) = \frac{\hbar N}{2} z(t) \tag{6}$$

we get

$$H = \langle \hat{H} \rangle = \frac{U}{\hbar^2} p_\theta^2 + \frac{\varepsilon}{\hbar} p_\theta - JN \sqrt{1 - \frac{4}{\hbar^2 N^2} p_\theta^2} \cos(\theta) \tag{7}$$

[1] A Smerzi, S Fantoni, S Giovanazzi, SR Shenoy Phys. Rev. Lett. **79**, 4950 (1997).

Semiclassical approximation

Under the assumption that the relative population imbalance is small ($|z(t)| \ll 1$) we get the **semiclassical** Josephson Hamiltonian[2]

$$H_J = \frac{U}{\hbar^2} p_\theta^2 + \frac{\varepsilon}{\hbar} p_\theta - JN \cos(\theta) \ . \tag{8}$$

The semiclassical dynamics of H_J is given by the Hamilton equations

$$\dot{\theta} = \frac{\partial H_J}{\partial p_\theta} = \frac{2U}{\hbar^2} p_\theta + \frac{\varepsilon}{\hbar} \tag{9}$$

$$\dot{p}_\theta = -\frac{\partial H_J}{\partial \theta} = -JN \sin(\theta) \tag{10}$$

It is possible to prove that this semiclassical Josephson Hamiltonian is reliable in the regime $N \gg 1$ with also $UN/J \gg 1$.

[2] K. Furutani, J. Tempere, LS, Phys. Rev. B **105**, 134510 (2022).

Semiclassical approximation

In the case of small oscillations around $z = 0$ and $\theta = 0$ from the corresponding linearized Hamilton equations

$$\dot{\theta} = \frac{\partial H_J}{\partial p_\theta} = \frac{2U}{\hbar^2} p_\theta + \frac{\varepsilon}{\hbar} \tag{11}$$

$$\dot{p}_\theta = -\frac{\partial H_J}{\partial \theta} = -JN\,\theta \tag{12}$$

one gets

$$\ddot{\theta}(t) + \omega_J^2\,\theta(t) = 0 \tag{13}$$

with **Josephson frequency**

$$\omega_J = \frac{\sqrt{2UJN}}{\hbar} \tag{14}$$

of harmonic oscillation around the balanced configuration.

Semiclassical approximation at finite temperature

At low energies the **equilibrium distribution** $f(p_\theta, \theta)$ of quantum-thermal states is essentially that of an harmonic oscillator with Josephson frequency ω_J, provided that $U > 0$. This distribution

$$f(p_\theta, \theta) = \frac{1}{\mathcal{Z}} \, e^{-H_J(p_\theta,\theta)/(k_B T_{\rm eff})} \qquad (15)$$

differs from the Maxwell-Boltzmann distribution by the fact that the temperature T of the bath is replaced by[3]

$$T_{\text{eff}} = \frac{\hbar\omega_J}{2k_B} \coth\left(\frac{\hbar\omega_J}{2k_B T}\right) \ , \qquad (16)$$

where $T_{\rm eff} \to T$ for $k_B T \gg \hbar\omega_J$ while $T_{\rm eff} \to \hbar\omega_J/2$ for $k_B T \ll \hbar\omega_J$. This provides us with a **semiclassical approximation** for the thermal averages of observables:

$$\langle \hat{O} \rangle = \frac{1}{\mathcal{Z}} \int_{-\hbar N/2}^{\hbar N/2} dp_\theta \int_{-\pi}^{\pi} d\theta \, O(p_\theta, \theta) \, e^{-H_J(p_\theta,\theta)/(k_B T_{\rm eff})} \ . \qquad (17)$$

[3] K. Furutani and LS, AAPPS Bull. **33**, 19 (2023).

Exact diagonalization: Thermal equilibrium

At fixed N, the diagonalization[4] of the $(N+1)\times(N+1)$ matrix associated to the **full Hamiltonian** $\hat{H}$ gives $N+1$ eigenvalues E_n and $N+1$ eigenstates $|E_n\rangle$. At thermal equilibrium with a bath of temperature T the density matrix reads

$$\hat{\rho} = \frac{1}{\mathcal{Z}} \sum_{n=0}^{N} e^{-E_n/(k_B T)} |\, E_n\,\rangle\langle\, E_n\,| = \sum_{i,j=0}^{N} \rho_{ij} |i\rangle_L |N-i\rangle_R \langle j|_L \langle N-j|_R \qquad (18)$$

where $|\, E_n\,\rangle = \sum_{i=0}^{N} c_i^{(n)} |i\rangle_L |N-i\rangle_R$ and

$$\rho_{ij} = \frac{1}{\mathcal{Z}} \sum_{n=0}^{N} e^{-E_n/(k_B T)} c_i^{(n)} (c_j^{(n)})^* \qquad (19)$$

The diagonal elements $\rho_{ii} = \langle |c_i|^2 \rangle = \sum_{n=0}^{N} |c_i^{(n)}|^2 e^{-E_n/(k_B T)}/\mathcal{Z}$ represent the average weights of the Fock states $|\, i, N-i\,\rangle$ in the statistical ensemble. Thermal averages are computed as

$$\langle \hat{O} \rangle = \mathrm{Tr}[\hat{\rho}\,\hat{O}] = \sum_{i,j=0}^{N} \rho_{ij} \langle\, i, N-i\,|\,\hat{O}\,|\,j, N-j\,\rangle \qquad (20)$$

[4] G. Mazzarella, LS, A. Parola, F. Toigo, Phys. Rev. A **83**, 053607 (2011).

Exact diagonalization: Thermal equilibrium

The ground state of the problem

$$|E_0\rangle = \sum_{i=1}^{N} c_i^{(0)} |i\rangle_L |N-i\rangle_R \tag{21}$$

is such that (with N even and $\varepsilon = 0$)

$$|E_0\rangle \to |\frac{N}{2}\rangle_L |\frac{N}{2}\rangle_R \tag{22}$$

for $U/J \gg 1$. This is the so-called **twin-Fock state**. Instead

$$|E_0\rangle \to \frac{1}{\sqrt{2}} \left(|N\rangle_L |0\rangle_R + |0\rangle_L |N\rangle_R \right) \tag{23}$$

for $U/J \ll -1$. This is the so-called **NOON state** (Schrödinger cat).
For $U = 0$ we have

$$|E_0\rangle = |ACS\rangle \tag{24}$$

with $|ACS\rangle$ the **atomic coherent state**, where the coefficient $c_j^{(0)}$ are Gaussian distributed around $i/N = 1/2$. For $N \to \infty$ we has $|ACS\rangle \to |GCS\rangle$ that is the **Glauber coherent state**.

Exact diagonalization: Thermal equilibrium

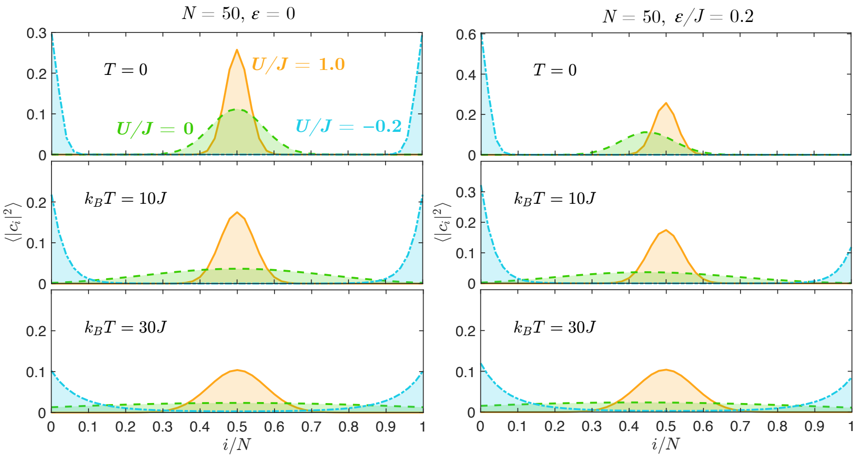

Thermal average $\rho_{ii} = \langle |c_i|^2 \rangle$ **of Fock weights** as a function of i/N , plotted for N $= 50$ and three values of U/J: 1 (solid orange line), 0 (dashed green line), -0.2 (dashed-dotted cyan line) at different temperatures T. **Left**: $\varepsilon/J = 0$; **right**: $\varepsilon/J = 0.2$.

Coherence visibility: Exact vs semiclassical

The coherence of our system can be characterized in terms of the quantity

$$\alpha = \frac{2\langle \hat{a}_L^\dagger \hat{a}_R \rangle}{N} \tag{25}$$

called **coherence visibility**.[5] This is related to the occupation of the single-particle ground state (**condensate fraction**) by

$$\frac{\langle \hat{a}_0^\dagger \hat{a}_0 \rangle}{N} = \frac{1+\alpha}{2} \tag{26}$$

where $\hat{a}_0 = (\hat{a}_L + \hat{a}_R)/\sqrt{2}$ and $\hat{a}_1 = (\hat{a}_L - \hat{a}_R)/\sqrt{2}$. Clearly, with (mean-field) Glauber coherent states one has always $\alpha = 1$.

Semiclassical method
By using the semiclassical approach, we obtain the formula

$$\alpha = \langle cos(\theta) \rangle = \frac{I_1(JN/(k_B T_{\text{eff}}))}{I_0(JN/(k_B T_{\text{eff}}))} \tag{27}$$

where $I_n(x)$ is the n-th modified Bessel function of the first kind.

[5] L. Pitaevskii and S. Stringari, Phys. Rev. Lett. **87**, 180402 (2001).

Coherence visibility: Exact vs semiclassical

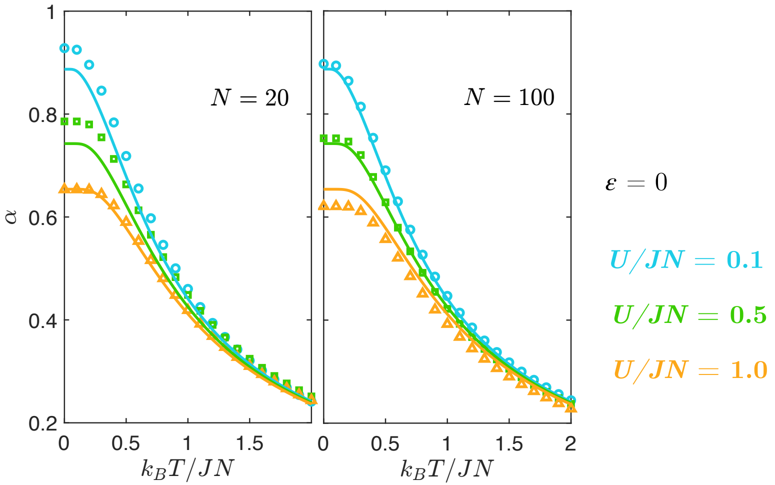

Coherence visibility α for $\varepsilon = 0$ as a function of $k_B T/JN$, plotted for $N = 20$ (**left panel**) and $N = 100$ (**right panel**), and three values of U/JN: 0.1 (cyan circles), 0.5 (green squares), 1 (orange triangles). The continuous lines are the corresponding semiclassical result.

Coherence visibility: Exact vs semiclassical

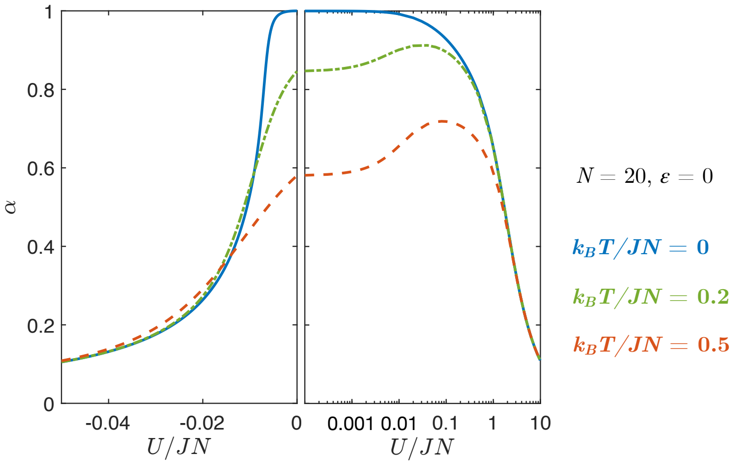

Coherence visibility α for $\varepsilon = 0$ as a function of U/JN, plotted for $N = 20$ and three values of $k_B T/JN$: 0 (solid blue line), 0.2 (dashed-dotted green line), 0.5 (dashed orange line).

Coherence visibility: Exact vs semiclassical

Introducing a small nonzero **asymmetry energy** ε, the coherence visibility α at $U = 0$ is significantly reduced both at zero and finite temperature T, while it remains almost unaffected for $|U|/JN > 0$.

In the repulsive regime the visibility α becomes a non-monotonic function of the interaction strength U at all temperatures (including $T = 0$), showing an initial increase before decreasing asymptotically to zero.

In the attractive regime the visibility α remains a monotonically decreasing function of the modulus of the interaction strength.

In the repulsive cases ($U > 0$) the **semiclassical approach** works quite well.

Population imbalance: Exact vs semiclassical

The **quantum population imbalance** can be measured by

$$k = \frac{1}{2}\left(\langle \hat{N}_L\rangle - \langle \hat{N}_R\rangle\right) \in [-\frac{N}{2}, \frac{N}{2}] \,. \tag{28}$$

In the semiclassical approach, with $\beta_{\rm eff} = 1/(k_B T_{\rm eff})$, we have

$$k = -\frac{\varepsilon}{2U} + \frac{e^{\beta_{\rm eff} N\varepsilon} - 1}{\sqrt{\pi U \beta_{\rm eff}}} \frac{e^{-\beta_{\rm eff} N^2 U(\varepsilon/NU+1)^2/4}}{\mathrm{erf}[\sqrt{\frac{1}{4}\beta_{\rm eff} N^2 U}(\frac{\varepsilon}{NU}+1)] - \mathrm{erf}[\sqrt{\frac{1}{4}\beta_{\rm eff} N^2 U}(\frac{\varepsilon}{NU}-1)]}$$

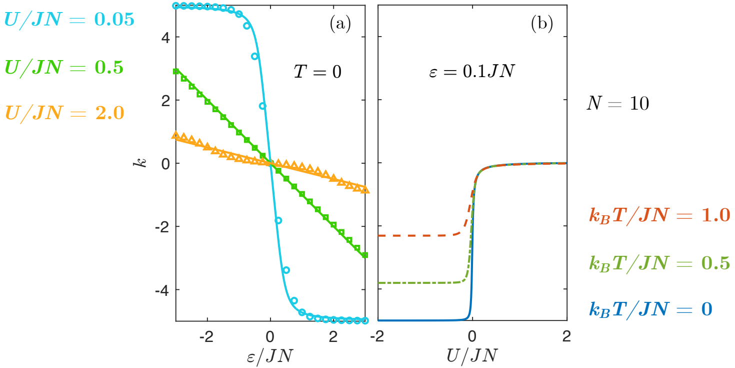

Entanglement entropy: Exact without semiclassical

The quantum entanglement between the two wells can be characterized [6] by considering the reduced density matrices

$$\hat{\rho}_L = \mathrm{Tr}_R[\hat{\rho}] \tag{29}$$

$$\hat{\rho}_R = \mathrm{Tr}_L[\hat{\rho}] \tag{30}$$

where $\hat{\rho}_L = \hat{\rho}_R$. In particular, the **entanglement entropy** is given by

$$S_E = -\sum_{i=0}^{N} \langle |c_i|^2 \rangle \ \ln\left(\langle |c_i|^2 \rangle\right) \qquad \in [0, \ln(N+1)] \tag{31}$$

that is nothing else than the von Neumann entropy S_{vN} of the two reduced density matrices: $S_E = S_{\mathrm{vN}}[\hat{\rho}_L] = S_{\mathrm{v}N}[\hat{\rho}_R]$.

[6] M. Le Bellac, A Short Introduction to Quantum Information and Quantum Computation (Cambridge Univ. Press, 2006).

Entanglement entropy: Exact without semiclassical

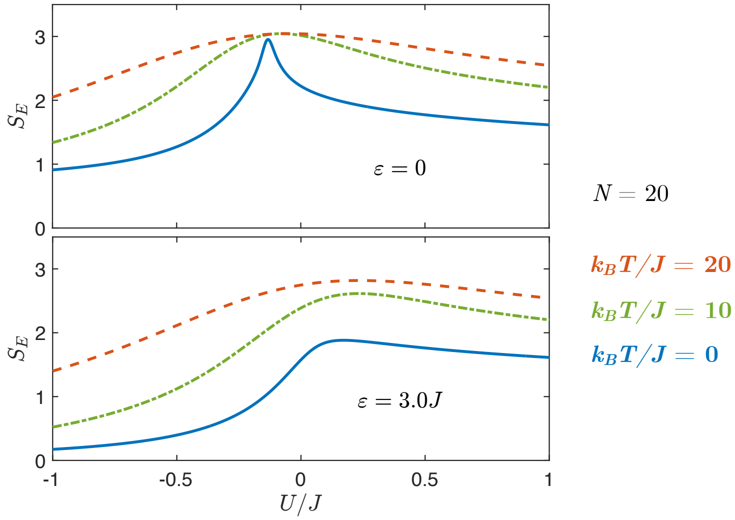

Entanglement entropy S_E as a function of U/J, plotted for $N = 20$ and three values of $k_B T/J$: 0 (solid blue line), 10 (dashed-dotted green line), 20 (dashed orange line). **Upper panel**: $\varepsilon/J = 0$; **lower panel**: $\varepsilon/J = 3$.

Conclusions

- We have characterized the thermal state of a bosonic Josephson junction by means of complementary observables (**coherence visibility**, **quantum population imbalance**, **entanglement entropy**), analyzing their dependence on the system parameters, showing how interparticle interaction, finite temperature, and on-site energy asymmetry affect their properties.
- We have also presented a **semiclassical description**, where thermal averages may be computed analytically (for $U > 0$) using a modified Boltzmann weight involving an effective temperature.
- The **semiclassical description** may be applied
  - ∗ to describe thermal properties of more complicated bosonic junctions (dipolar interactions, multi-component);
  - ∗ to investigate quantum dissipative systems.
- Our results are published in the paper:
  C. Vianello, M. Ferraretto, and LS, Phys. Rev. A **111**, 063310 (2025).

Thank you for your attention!